Version of Record: https://www.sciencedirect.com/science/article/pii/S0045653521003556
Manuscript_16fb335e718130cef36d2ed986287455

Quantification and composition of microplastics in the Raritan Hudson Estuary: comparison to pathways of entry and implications for fate

AUTHORS: Kendi Bailey,[1] Karli Sipps,[2] Grace K. Saba,[3] Georgia Arbuckle-Keil,[2] Robert J. Chant,[3] N.L. Fahrenfeld[1]*

[1]Civil & Environmental Engineering, Rutgers, The State University of New Jersey, Piscataway, NJ; [2]Chemistry, Rutgers, The State University of New Jersey, Camden, NJ; [3]Department of Marine and Coastal Sciences, Rutgers, The State University of New Jersey, New Brunswick, NJ

*nfahrenf@rutgers.edu; (P) 848-445-8416; 500 Bartholomew Rd., Piscataway, NJ, 08854

Abstract

Comprehensive approaches are needed to understand accumulation patterns and the relative importance of pathways of entry for microplastics in the marine environment. Here, a highly urbanized estuarine environment was sampled along a salinity gradient from the mouth of the Raritan River, (New Jersey, USA) and into the Raritan Bay and the coastal ocean which are further influenced by discharge from the larger Hudson River. Polymers were characterized in two size classes by FTIR and/or Raman spectroscopy. The highest concentration of 500-2000 μm microplastic particles were observed in the mouth of the Raritan during summer low flow conditions, whereas the 250-500 μm microplastic particles were more prevalent in the bay and coastal ocean samples. These results were interpreted using fragmentation and mixing models to provide insight into the sources and fate of microplastics in this estuarine/coastal region. To investigate the potential pathways of entry into the system, samples were collected from various hydraulically connected storm water outfalls and the influent and effluent of wastewater treatment plants and polymer concentrations and types were compared to the estuarine samples. The concentrations of microplastics (500-2000 μm) ranged from 400-600 microplastics/m^3 in storm water compared to <1-2.75 microplastics/m^3 across the estuary. Of interest for analysis is the observed linear correlation between the total concentration of particles in a sample following oxidation and density separation and its microplastic concentration. Overall, the results presented reveal potentially important sources of microplastics in the estuarine environment and have implications for understanding the behavior, transport, and fate of microplastics under varying flow conditions and from estuaries with variable flushing times.

Keywords: microplastic; estuary; river plume; FTIR; wastewater; storm water

1. Introduction

Plastics from micro (<5mm) to macro sizes are frequently observed marine debris (Galgani et al., 1996; Cózar et al., 2014), and rivers are considered a major source.(Andrady, 2011; Morritt et al., 2014; Rech et al., 2014; Wagner et al., 2014; Cheung et al., 2016) Pathways for entry into riverine environments have received varying attention with a major emphasis on effluent from municipal wastewater treatment plants (Talvitie et al., 2015; Estahbanati and Fahrenfeld, 2016; Mason et al., 2016) and lesser focus on storm water that can carry debris from land application of sewage sludge, tires, construction activities, artificial turf, littering, etc. (Magnusson et al., 2016). Marine microplastics also come from atmospheric deposition (particularly for fibers)(Pirc et al., 2016), boating and fishing activities (Magnusson et al., 2016), and import from other land-based sources as evidenced by plastic accumulation in remote environments (Convey et al., 2002). Documenting the composition of estuarine plastic debris compared to different sources/pathways (Fahrenfeld et al., 2019) and understanding spatial controls on microplastics in estuaries may inform management practices focused on mitigation strategies that target sources and/or locations where plastics accumulate.

Of particular interest is the spatial variability and behavior of microplastic particle sizes given that the majority of microplastics in the marine environment are “secondary microplastics” that result from fragmentation of larger plastic debris by mechanical abrasion, UV photodegradation, or biodegradation (Alimi et al., 2018). Mass balance estimates indicate plastics released to the ocean in recent decades are 100 times larger than the floating inventory suggestive of a significant loss term (Cózar et al., 2014). The size class of microplastics observed in ocean gyres indicate that microplastic particle concentrations are lower than expected at the 1-2 mm scale (Cózar et al., 2014), a size class analyzed in this study. Among the leading candidate processes

47 for the loss term that would be most active at this size class are ballasting (i.e., sinking) due to
48 biofouling and ingestion by small marine organisms such as zooplankton (Cózar et al., 2014).

49 These processes driving the loss term in the ocean gyres are more active in the biologically
50 productive coastal ocean. Moreover, we expect the greatest likelihood of primary uptake and of
51 biofouling to occur where elevated microplastic and plankton concentrations, and their encounter
52 rates, are elevated: frontal environments which are a common feature of river plumes (Garvine
53 and Monk, 1974). River plumes are associated with elevated biomass, partly due to the
54 concentration of material by converging flows (Garvine and Monk, 1974; O'Donnell et al.,
55 1998), and the influx of nutrient-rich waters that support biomass growth (Franks, 1992). Marine
56 debris has been associated with such convergence zones (Howell et al., 2012) outside of coastal
57 regions and ingested microplastics in zooplankton were correlated with microplastic
58 concentrations in marine waters (which in Northeast Pacific Ocean were highest nearest to land)
59 (Desforges et al., 2015). River plumes areas are also important areas of activity for marine
60 vertebrates (Scales et al., 2014). In addition, buoyant plumes originate from highly turbulent and
61 productive estuaries where production of secondary microplastics may be significant due to
62 mechanical breakup in shallow estuaries. Where biofouling is intense and microplastics will
63 interact with bottom sediments during quarter-diurnal tidal mixing events and may be
64 periodically stranded on shorelines by the rise and fall of the tide.

65 The objectives of this study were to (1) quantify microplastic concentrations in surface water to
66 relate patterns of microplastic concentration and size-class distribution to hydrographic features
67 in river plume dominated regions, (2) relate these patterns and distributions to the multiple
68 watersheds influencing this region, and (3) investigate potential sources of microplastics by
69 quantifying microplastic concentration and clustering polymer types in wastewater influent,

effluent, and storm water. Notably, untreated wastewater influent can be released at the mouth of the Raritan and throughout the estuary from dozens of combined sewer outfalls during rain events. Results presented provide insight into sources and fate of microplastics in this estuarine system and can be used to inform mitigation strategies (if and where needed).

2. Materials & Methods

Paired microplastic and hydrographic sampling were performed that extended from the fresh-water end member of the Raritan River to the coastal ocean. This section is also influenced by discharge from the Passaic, Hackensack and Hudson Rivers (Chant et al., 2008b). Sampling occurred during a relatively dry period in July 2018 and following a heavy precipitation event in in April 2019. Potential pathways of entry (from here out called "sources" for simplicity) were sampled during the study period including wastewater influent, effluent, and storm water from hydraulically connected locations (where possible) for comparison.

2.1 Study Site

Hudson-Raritan Estuary has many potential sources of plastics from a number of highly urbanized watershed. The Hudson-Raritan Estuary is bound by Staten Island, New York to the North and New Jersey to the South (Figure 1). The Arthur Kill connects Raritan Bay to Newark bay to the North which is then connected to New York Harbor via the Kill van Kull. The mean flow in these Kills is counterclockwise with a mean transport of 300 m^3/s that is significantly modulated by wind forcing (Chant, 2002). The bay is influenced by multiple rivers all with dense human populations. The Raritan River, with a mean discharge of 35 m^3/s and 1.2 million people in its watershed, enters the bay from the west. The Passaic and Hackensack rivers, with mean discharges of 33 m^3/s and 2 m^3/s and populations of 2.5 million and ~1 million,

respectively, flow into Newark Bay. A portion of this discharge flows south in the Arthur Kill into Raritan Bay, while the remainder flows into New York Harbor through the Kill van Kull where it mixes with waters from the Hudson River. The Hudson River, with a mean discharge of 800 m^3/s and watershed population of 8 million, enters Raritan Bay from the east and recirculates in the bay prior to debouching to the coastal ocean (Choi and Wilkin, 2007). The Hudson's discharge penetrates most deeply into the bay during easterly winds (Choi and Wilkin, 2007; Hunter et al., 2010). Moreover, discharge from New York Harbor also incorporates waters from western Long Island Sound through the East River which also contains large population centers. In addition, several other smaller rivers in highly urbanized regions also contribute to the fresh water and plastics budget of Raritan Bay.

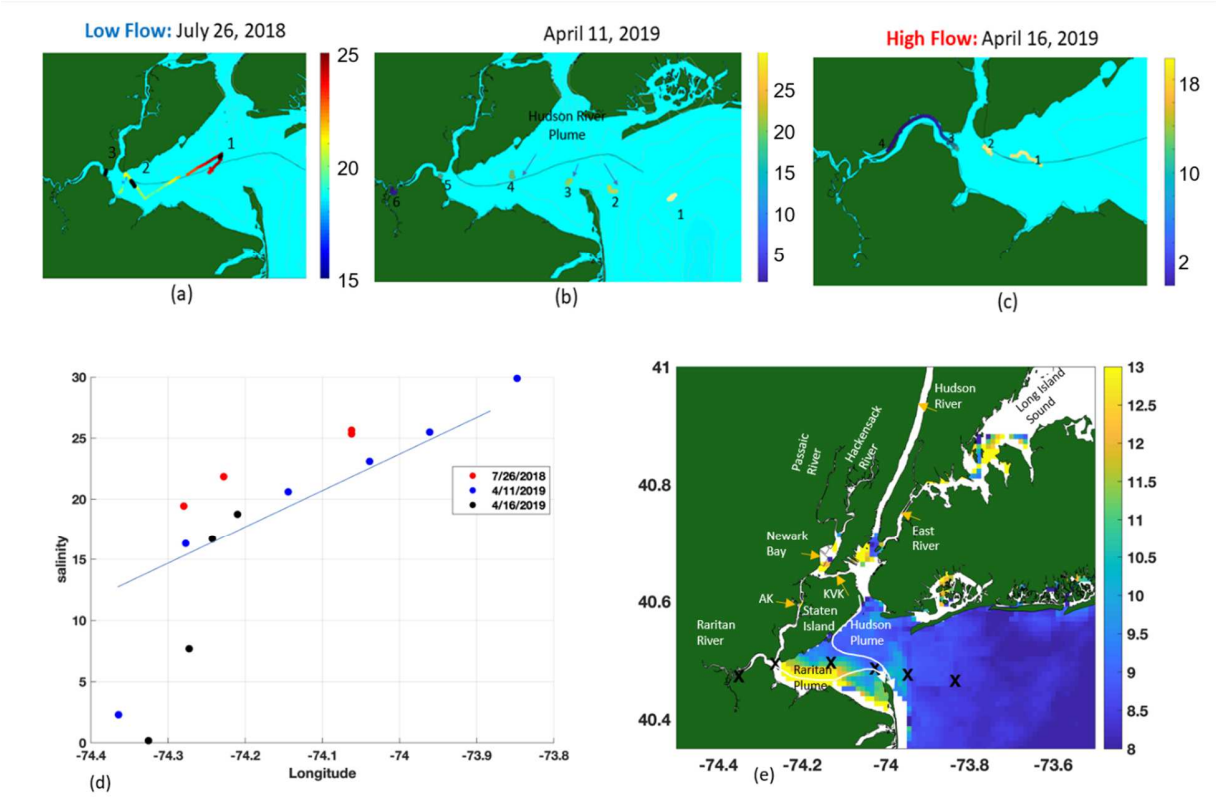

Figure 1 –Surface water sampling sites (a) July 26, 2018 (low flow) (b) April 11, 2019 (moderate flow) (c) April 16, 2019 (high flow). The colors represent surface salinity from low (blue) to high (dark red). (d) Surface salinity (e) and study region and station locations from April 11, 2019 overlaid on sea surface temperature obtained from MODIS on April 11th, 2019.

2.2 Sampling Methods & Environmental Conditions

Surface water sampling was performed along a salinity gradient from the Raritan River and through Raritan Bay to the coastal ocean (Fig. 1). Sampling sites were selected to span a maximum range of salinity space given time and weather constraints of each day. Samples were collected aboard the R/V Rutgers vessels boat 20.3cm diameter plankton nets (mesh size 80 or 150 µm, Science First, Yulee, FL) in duplicate at each of three to six sampling locations on July 26, 2018 (low flow), April 11, 2019 (moderate flow), and April 16, 2019 (high flow). Raritan River discharge was highest during the April 16, 2019 survey and peaked at a daily mean flow of 157 m^3/s one day prior. While river discharges were low on both April 11, 2019 and July 28, 2018 with daily mean flows of 21 m^3/s and 25 m^3/s respectively, the July 2018 survey followed an extremely dry period where discharge the previous 30 days averaged 10.9 m^3/s compared to 53.3 m^3/s in the 30 days prior to the April 11, 2019 survey. Hudson river discharge was low (~300 m^3/s) during the 2018 survey and high (1000 m^3/s -2000 m^3/s) during the 2019 surveys. The elevated river flow in 2019, particularly that from the Hudson resulted in lower salinities in the Bay in 2019, which were 3-4 psu lower relative to 2018 (Figure 1d). However, the along bay salinity gradients on both days were similar and varying approximately 1 psu every 2.5 km.

The nets were fixed to the back of the vessel to collect surface particles by towing for 20 minutes at a vessel speed of 2 knots. The volume passed through the net was either calculated using the speed of the boat, the time towed, and the net dimensions or via measurements from flow meters

placed at the center of the net opening (General Oceanics, Miami, FL). One blank (net left open to air for the length of one tow) and one matrix spike (replicate net towed then spiked with polyethylene beads extracted from a personal care product), were collected at one site on each April 11, 2019 and April 16, 2019.

Five wastewater treatment plants (WWTPs) were sampled in New Jersey, two of which were hydraulically connected to the study area. Either composite or grab samples were collected from wastewater treatment plants based upon availability (Table A1). Notably, plankton nets were not used for these or the storm water samples to avoid clogging of the mesh.

Storm water samples were collected from three sites during heavy rain on October 16, 2019 (Fig. A1). Sample sites included two pipes carrying runoff from urban areas in Bayonne and New Brunswick, NJ and one site carrying storm water from a recreational area in Piscataway NJ (labelled City B, City N, and Field P, respectively). City B samples were collected as pump out of a storm drain and come from a combined sewer system. Field P and City N samples were taken from the pipe outfall and are part of the storm water pipes in a region with separate sanitary systems. Five liters of storm water were collected over the duration of a rainstorm with one liter taken every 10-45 min at a time per site (Fig. A2). Rainfall and stream gage data were collected from the nearest stations for each sampling area. Rainfall data were obtained from Rutgers New Jersey Weather Network (Rios et al., 2010), and stream gage data were obtained from United States Geological Survey (USGS).

2.3 Microplastic Extraction Methods

After sample collection, nets were rinsed with DI water and separated via wet-sieving into size classes using a series of standard soil sieves (2000, 500, 250 μm size). Material retained on the

2000 µm sieve size was discarded. The material collected in each remaining sieve was rinsed with DI water and transferred to individual glass beakers. The organic matter was oxidized by hydrogen peroxide and a catalyzed iron (II) solution (Masura et al., 2015). Briefly, 20 mL of 0.05 M iron (II) solution was added to each beaker, followed by 20 mL of 30% hydrogen peroxide. The solutions were heated to 75°C on a hot plate and then stirred using a magnetic stir bar for 30 minutes before sodium chloride (NaCl, 6 grams per 20 mL), was added to increase the mixture density. The oxidized and NaCl treated samples were transferred to glass funnels with the ends capped by clamped surgical tubing for density separation. The funnels were covered with foil to prevent contamination and left overnight for settling. Settled materials were discarded and the floating particles were collected, rinsed with DI water, and transferred to glass petri dishes covered with a glass lid.

2.4 Chemical Analysis & Spectral Interpretation

The recovered particles in the 500-2000 µm size range were analyzed using Attenuated Total Reflectance (ATR) Fourier Transform Infrared (FTIR) spectroscopy on one of two instruments. The first instrument was a Bruker Alpha spectrometer (Bruker Optics, Billerica, MA) with a single bounce diamond or germanium internal reflection element (IRE) ATR accessory and a DTGS (Deuterated Triglycine Sulfate) detector. The other FTIR was a PerkinElmer Spectrum 100 spectrometer (PerkinElmer Life and Analytical Sciences, Shelton, CT) equipped with a 3-reflection diamond ATR accessory and a DTGS detector. Particles were transferred to the surface of the IRE using tweezers. A spectrum was collected for each particle in the wavenumber region of 4000- 600 cm^{-1} averaging 32 scans at 4 cm^{-1}. For samples containing less than 80 particles, all particles were analyzed. For samples containing greater than 80 particles, up to 119 particles were analyzed starting with visually identified microplastic. Microscope images were

collected for select samples using a reflected light microscope (Stereo Zoom Microscope, Olympus, Japan) and images were captured via cell phone camera.

FTIR spectra of common polymers such as polyethylene (PE) and polypropylene (PE) were analyzed via comparison with known spectra and confirmed using SiMPle (Systematic Identification of Microplastics in the Environment) (Primpke et al., 2018). SiMPle is a program that matches sample spectra with a reference database providing a probability (match quality) score. For this study, polymers with probability scores over 50% are counted as plastics and labelled by their polymer identification and those with score 40-50% were manually interpreted to determine if the particle was likely to be microplastic.

Total recovered particles (following oxidation and density separation) in the 250-500 μm size range were enumerated under a stereomicroscope prior to spectral analysis. For samples containing less than 50 particles, all were analyzed, providing quantitative results on microplastic concentration and qualitative description of polymer types. For samples containing greater than 50 particles, a subset of the total particles was analyzed up to 133 particles, starting with visually identified microplastic, providing qualitative description of polymers observed and a lower bound for microplastic concentration.

Particles were analyzed using a combination of FTIR and Raman microscopy. FTIR spectra were collected on a Bruker LUMOS FTIR microscope, equipped with an 8x microscope objective and liquid nitrogen-cooled mercury cadmium telluride (MCT) detector. Spectra were collected in the wavenumber region of 4000-700 cm^{-1} with 64 background scans and 64 sample scans at a resolution of 4 cm^{-1}. Thin, film-like samples were primarily measured in transmission mode on a calcium fluoride (CaF_2) substrate, while samples that were not IR transmissive were

194 measured in reflectance mode on a MirrIR slide (Kevley Technologies, Chesterland, Ohio).
195 Raman spectra were collected on a Horiba XploRA PLUS Raman microscope, equipped with
196 532, 638 and 785nm excitation wavelengths and 10x [numerical aperture (N.A.) = 0.25], 50x
197 LWD (N.A. = 0.50) and 100x (N.A. = 0.90) microscope objectives. Measurement parameters
198 were adjusted for each sample in order to optimize the signal-to-noise ratio and mitigate any
199 unwanted effects, such as fluorescence interference. Spectra were interpreted manually based on
200 chemical functional group correlations and also evaluated using BioRad's KnowItAll software,
201 as well as siMPle. When a specific match could not be produced, samples were broadly
202 categorized based on the functional groups present in the microplastics.

203 ***2.5 Data Analysis***

204 Statistical analysis was performed using R (www.rproject.org). A Shapiro-Wilk test was used to
205 test for normality of total particle and microplastic concentration data. Given that data were not
206 normal, a Kruskal-Wallis test was applied to compare the microplastic concentrations observed
207 at different surface water sampling sites and dates (separately for the 250-500 μm and 500-2000
208 μm data), followed by a posthoc pairwise.t.test with a Bonferroni correction for multiple
209 comparisons. The same tests were used to determine differences in concentration by sample
210 source (500-2000 μm data only). Total particles following oxidation and density separation and
211 microplastics in the small and large size class were compared by a paired Wilcoxon rank test.
212 Correlation between the total concentration and the microplastic concentration per cubic meter
213 was plotted as a linear regression and significance tested with a Spearman rank-order correlation
214 test. Percentages of polymer types were found by separating the polymer hits into categories by
215 polymer class. The categories used were polyethylene, polypropylene, polystyrene, polyester,
216 rubber, vinyl copolymers, and other plastics. The polymer types and concentrations for the 500-

2000 µm particles were compared between samples by creating a Bray-Curtis dissimilarity matrix of square root normalized data followed by cluster analysis with a SIMPROF test.

3. Results

3.1 Microplastic concentrations in estuarine waters

Microplastics were observed in every sample type (surface water, storm water, wastewater). In surface water samples, microplastic concentrations for the 500-2000 µm particles were the highest in the river and lowest in the samples collected in the highest salinity water where Raritan Bay meets the coastal ocean (Fig. 2). Differences were observed between the different sites/dates ($p=0.033$, Kruskal-Wallis), primarily due to the high observation at the mouth of the Raritan River during the July sampling event which was significantly higher than concentrations observed at all sites on the other sampling dates (all $p \leq 0.028$, posthoc pairwise.t.test). However, there were no significant differences observed between samples taken on the same day (all $p \geq 0.81$, posthoc pairwise.t.test). The relative percent difference between replicate samples ranged from 0-200% with an average of 94.8+/-84.2%. It is worth noting that the samples with higher relative percent differences (RPDs) among replicates were those with low microplastic concentration (i.e., <5 particles/cubic meter). For samples with >5 microplastics/cubic meter, RPD was 34+/-28%. The average recovery of microplastics in matrix spikes was 68.8±5.3%. There were no microplastics observed in the field blank samples.

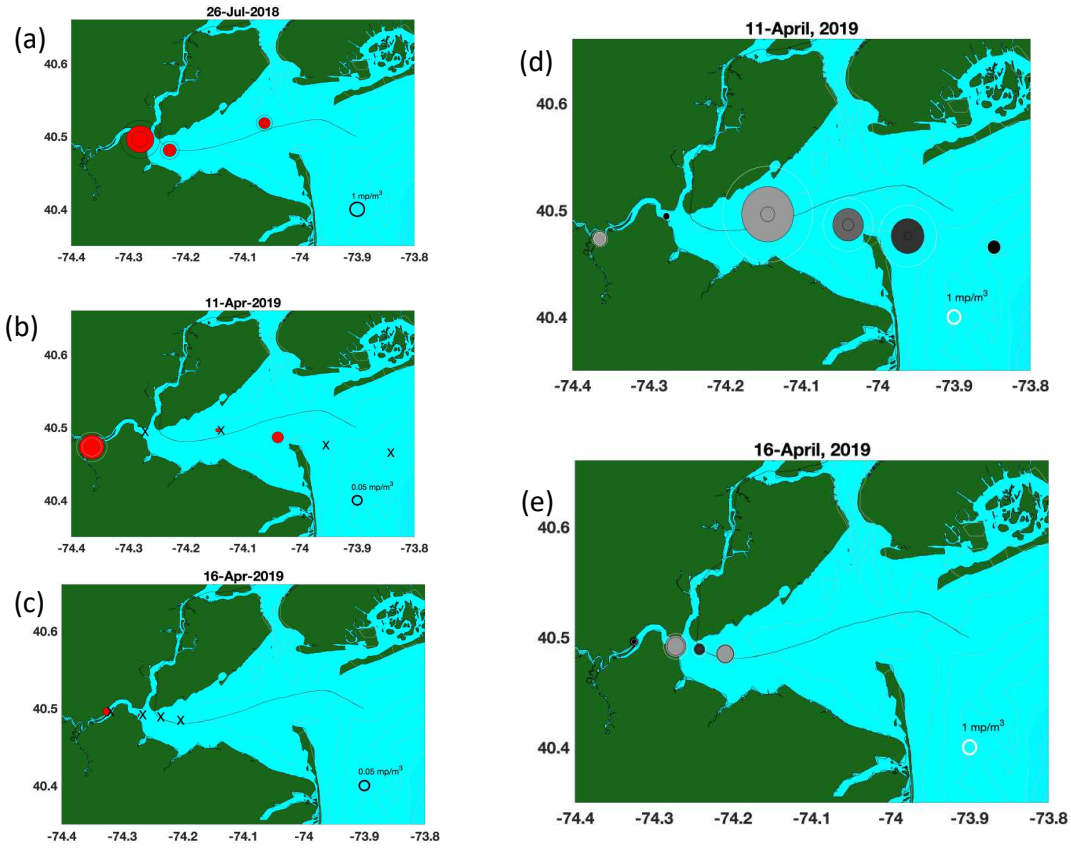

Figure 2 - Maps of the sampling area and bubble plots showing the average concentration of large (a,b,c) and small (d,e) microplastics per cubic meter on noted sampling dates. When microplastics were observed in both replicate samples, the overlaid circles on the bubble plots indicate the high and low values and X's represent samples for which microplastics were not detected. For the large microplastics, all data shown were measured. For the small microplastics black dots indicate both samples were analyzed, dark grey only 1 of the replicates was analyzed and light grey estimated using the correlation shown in Figure 3.

Next, to understand if microplastic observations were correlated with total particles present in the sample following wet peroxide oxidation and density separation, a correlation was tested between the total concentration of particles and the microplastic concentration per cubic meter showing a significant positive correlation in surface water samples (linear regression: slope=0.56, R^2=0.9798, p= 2.58×10^{-9}, Spearman Rank, Fig. 3).

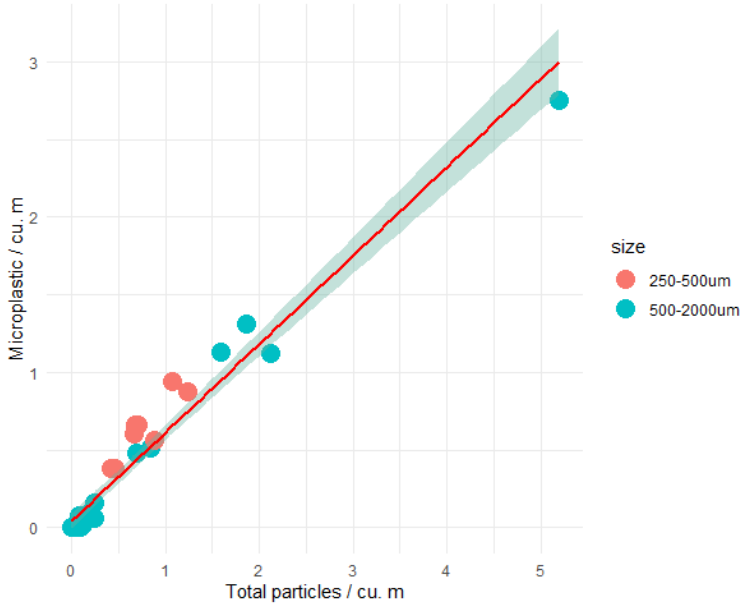

Figure 3 - Relationship between total concentration of particles per cubic meter and the microplastic concentration per cubic meter for surface water samples. Total particles refer to particles remaining following sieving, wet peroxide oxidation, and density separation. the red line on the graph represents the linear regression and the shaded area around it represent a 95% confidence interval.

Analysis was also performed on samples from the April sampling events for particles in the 250-500 µm size range. There were more total particles following oxidation and density separation in the smaller size class (1.88±2.00 total particles/m^3) compared to the larger size class (0.19±0.46 total particles/m^3, $p=1.91\times10^{-6}$, paired Wilcoxon rank test). This resulted in 21-421 total particles per sample (94.2±100 particles/sample) to analyze in the smaller size class, the higher range of which was not practical to completely analyze using the methods applied here. All particles were analyzed for three sites for both replicates (N=6/14) with RPD between replicates of 32.9±24.1%. All particles were analyzed for one replicate from two sites (N=2/14). There were significantly more microplastics for the smaller size than the larger particles ($p=1.91\times10^{-6}$, paired Wilcoxon rank test). Again, the correlation between total and microplastic particles were analyzed including the samples with 100% of particles analyzed from both size classes resulting in a strong significant correlation ($R^2=0.97$, $p < 2.2\times10^{-16}$, Spearman rank).

For the remaining 250-500 μm samples, 20-133 particles were analyzed, representing 10.7% (for the 421-particle sample) to 52.6% (for a 57-particle sample) of total particles to provide a lower bound for microplastic concentration and a qualitative description of the polymers observed. Using the regression described immediately above, the concentration of 250-500 μm microplastic particles in the partially analyzed samples were estimated. Combining the measured and estimated concentrations for the 250-500 μm size class, there were significantly more microplastic in the smaller than the large size class ($p=9.53\times10^{-5}$, paired Wilcoxon test). Although, there were no significant site-to-site differences in microplastic concentrations for the smaller size class (p=0.25, Kruskall Wallis test), the highest microplastic concentrations for the small size class were located near the center of Raritan Bay (in moderate salinities) rather than at the mouth of the Raritan River as was observed for the larger size class.

3.2 Comparison of estuarine waters and source water microplastic

Microplastics were measured in source waters for the 500-2000μm size class. The wastewater influent had the highest concentrations of microplastic compared to wastewater effluent, storm water, and surface water (all $p\leq 6.5\times10^{-5}$, posthoc pairwise.t.test with Bonferroni correction; Fig. 4). The wastewater influent also had the greatest range in concentrations, spanning two orders of magnitude. Wastewater effluent, storm water, and surface water had similar concentrations of microplastics (all $p\geq0.23$, posthoc pairwise.t.test with Bonferroni correction) (Fig. 4). However, the sample size for storm water (N=3) was small and a larger sample size could possibly result in significant difference in microplastic concentration compared with surface water (N=26). These matrices had median concentrations of 600 microplastics/m^3 (storm water) and 0.01 microplastics/m^3 (surface water) the difference likely due to dilution of the storm water after release to the receiving water.

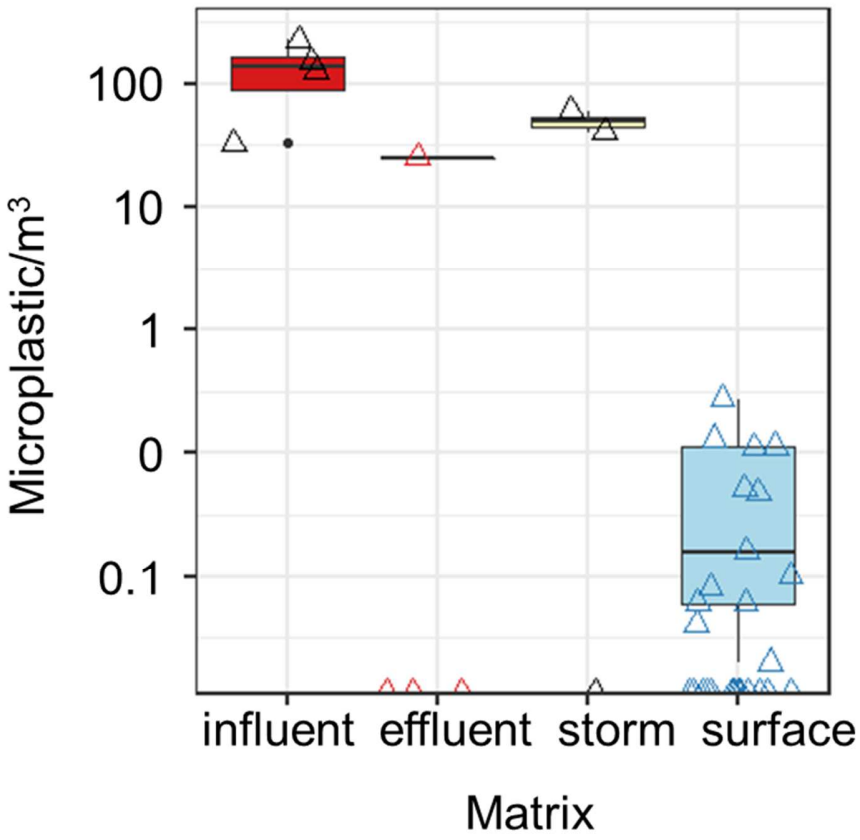
100
10
1
0
0.1
Microplastic/m3
influent
effluent
storm
surface
Matrix

291

Figure 4 – Boxplot with jitter (open triangles) of 500-2000 μm microplastic concentration on log scale of wastewater influent ("influent," N= 4), wastewater effluent ("effluent," N=4), storm water (N=3), and surface water (N=26). Data points intersecting the x-axis had <1 microplastic per cubic meter.

The correlation between total particles and microplastic was tested on the data from all the fully analyzed samples and showed a positive correlation across all sampling types (linear regression: 0.34, R^2=0.93, p=1.15×10^{-9}, Spearman Rank, Fig. 3). The field blanks for both the surface water and wastewater sampling did not have any microplastic particles, but the field blanks for the wastewater samples each had one non-microplastic particle. This low level of non-microplastic contamination did not appear to impact the correlation result.

3.3 Microplastic composition in surface and source waters

A variety of polymer types were identified via the SiMPle analysis, and example spectra associated with select microparticles are shown in Fig. S4. For the microplastics in the 500-2000 μm samples, the most commonly observed was polyethylene which represented 45.1±32.9% of microplastics identified (all p<0.0003, posthoc pairwise.t.test with Bonferroni correction) and was observed in 13/15 samples with microplastic (Fig. 5a). This was also the most prevalent polymer type observed in the smaller size class. Polymers including rubber, polypropylene, polystyrene, polyester, and various vinyl copolymers were also present. The vinyl copolymers consisted of ethylene ethyl alcohol, ethylene vinyl alcohol, styrene allyl alcohol, and styrene acrylonitrile. Polymers categorized as "other" included turf fibers, polyether, and polyvinyl stearate.

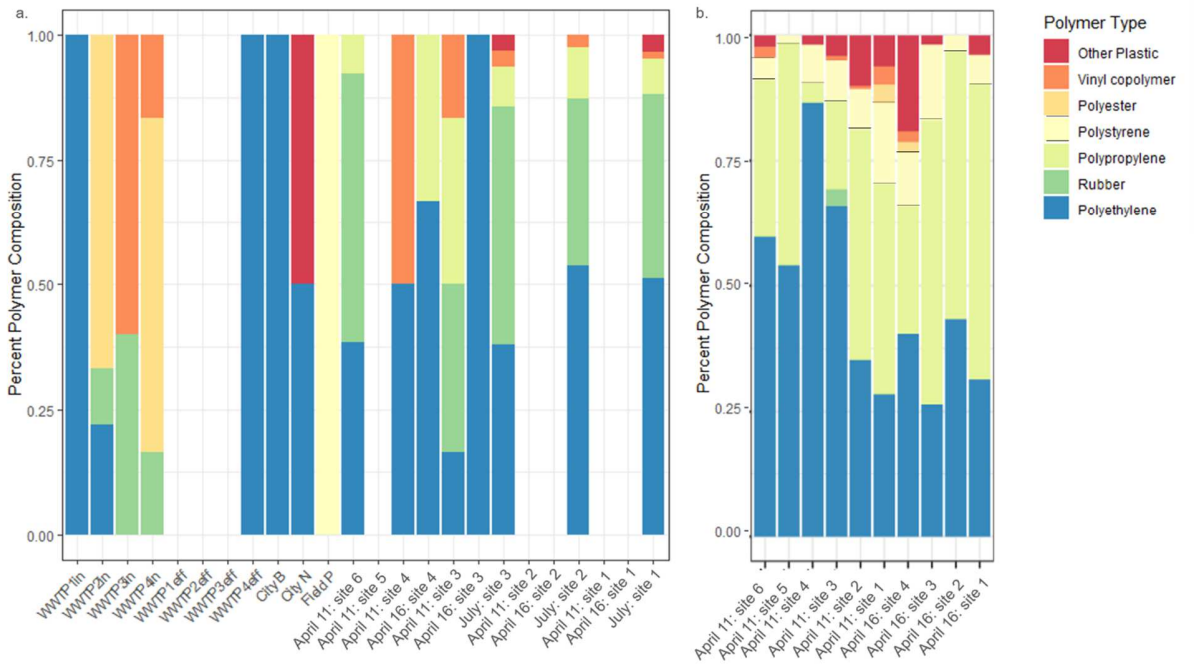

315

316

317 ***Figure 5*** - The polymer type composition of each sample for the (a) 500-2000 µm and (b) 250-
318 500 µm particles (fragments, pellets, sheets)

319 Cluster analysis was used to understand if there were patterns in the polymer type and
320 concentration observed for the 500-2000 µm particles between the different sample types and
321 locations (Fig. A5). No clusters were significantly different (SIMPROF test, $p>0.196$).
322 Replicate surface water samples clustered with 30.6-71.4% similarity, which did not necessarily
323 result in them forming clusters with the highest similarity to one another. Surface water samples
324 from the low flow July 26, 2018 sampling formed a cluster with 59.1% similarity with one
325 another and cluster with select samples from the April 11, 2019 moderate flow sampling at
326 30.6% similarity. Samples from Sites 3 and 4 on the low flow sampling clustered with
327 wastewater influent from plants 2-3 with 42.0% similarity. The high flow April 16th samples
328 with MP clustered with influent from WWTP1, effluent from WWTP4, and storm water from

City N and B with 63.4% similarity. Field P was the most distinct sample, consisting of only polystyrene with 0% similarity to the other samples.

4. Discussion

4.1 Microplastic in the Raritan river and estuary

Microplastic concentrations between 0 and 2.75 microplastic/m^3 for 500-2000µm and 0.38 (measured) to 4.71 (estimated) microplastic/m^3 for 250-500µm were observed in surface waters collected from the mouth of the Raritan River out to the coastal ocean. This is consistent with the range reported in a recent review of microplastics and nanoplastics in aquatic environments that concluded that the concentrations of macro and microplastics in lakes, rivers, and oceans would be between 10^{-3}-10^{3} microplastic/m^3 (Alimi et al., 2018). Likewise, the values found are consistent with studies of estuarine and coastal environments from the Raritan River (Estahbanati and Fahrenfeld, 2016), Delaware Bay (Cohen et al., 2019), Pearl River estuary (Cheung et al., 2018; Lam et al., 2020), Tamar Estuary (Sadri and Thompson, 2014), and the Adriatic Sea (Atwood et al., 2019) that reported values of 0.028-84 microplastic/m^3. Higher concentrations per volume were reported when smaller size classes were included resulting in a larger range of particle sizes (Hitchcock and Mitrovic, 2019; Wu et al., 2019; Zhang et al., 2019).

The highest concentration of 500-2000 µm microplastic was found at the mouth of the Raritan River and in the river itself, as compared to the coastal ocean. A similar observation was reported in previous studies of microplastic size classes 300-5000 µm (Cohen et al., 2019), >500 µm (Atwood et al., 2019), >125 µm (Schmidt et al., 2018) in the river and ocean environment suggesting the river is a source that is diluted as it enters the estuary. In contrast, the highest estimated MP concentrations for the 250-5000 µm samples were located in the mid-Raritan Bay

in the vicinity of the Hudson River plume. Implications of these observations are discussed in Section 4.3.

There were generally no significant differences in samples taken on the same day with the exception of the 500-2000 µm samples mouth of the Raritan River during the July sampling event which was higher than all other concentrations observed in that size class. There were, however, noticeable differences for the larger size particles between flow conditions where July (low flow) had microplastic concentration 1.22+/-0.826 microplastic/m^3, April 11 (moderate flow) had 0.35+/-0.052, and April 16 (high flow) had 0.01+/-0.0214. Kapp et al. also found that periods of low flow may accumulate microplastic particles (Kapp and Yeatman, 2018) greater than 100 µm after sampling the Snake River, WY and revealing a negative correlation between microplastic concentration and velocity of water. In low flow conditions, higher concentrations were observed likely because microplastics were not diluted by rain and runoff and had the opportunity to concentrate in the estuary due to reduced flushing. This is consistent with the long period of low flow conditions in the Raritan prior to our July 28th survey that allowed microplastics to accumulate in the Raritan basin before being flushed out of the river, and low concentrations of microplastics region-wide after a heavy precipitation event and likely dilution (April 16, 2019). Indeed, the low flow sampling on July 28th, 2018 was a discharge higher than any flows in the prior 40 days. In contrast, the moderate flow sampling on April 11th, 2019 occurred following a large flushing event that had a peak flow on March 22nd, 2019 of 219 m^3 and decreased monotonically until early April when it leveled off at 20 m^3/s (Figure 6). Rainfall events have been associated with elevated microplastic concentrations in eastern Australian estuaries (Hitchcock and Mitrovic, 2019), and estuarine rivers feeding the Chesapeake Bay (Yonkos et al., 2014).

374 The most commonly observed polymer in the river and estuary was polyethylene, polyethylene
375 and polypropylene have been commonly observed as prevalent polymer types in other estuarine
376 waters (Sadri and Thompson, 2014; Cheung et al., 2018; Wu et al., 2019; Zhang et al., 2019;
377 Lam et al., 2020; Nel et al., 2020). The microplastic analyzed here were fragments, films, and
378 pellets but the observed morphologies were not quantitatively categorized. Fibers were observed
379 in the samples but were not analyzed because of their small size and the chance of
380 contamination.

381 There was a linear correlation between the total particle concentration remaining after the
382 oxidation and density separation and microplastic concentration across sampling sites. The
383 particles not classified as microplastic (i.e., manmade polymers) had high similarity to cellulose,
384 natural fibers, cow fur, shells, and other natural materials. Notably, the wastewater effluent had
385 several samples with a microplastic concentration of <1 particle per sample but that did contain
386 other particles and therefore fell well outside of the regression confidence interval. The lower
387 microplastic concentration may be due to sampling at a relatively small volume, or WWTPs
388 being effective at removing microplastic. While some papers sample a small percentage of
389 sample and scale up the results, little is known about the relationship between the total
390 concentration of particles and the microplastic concentration in a sample. This result may
391 indicate that total post-oxidation and density separation particle counting, and a regression could
392 be used to estimate microplastic concentration in surface water, wastewater influent, and storm
393 water, but not wastewater effluent. Given that microplastic analysis with the techniques applied
394 here is not high throughput, application of regression could help provide a first estimate of total
395 microplastic concentration in such samples and help reduce analysis time. Of course, validation
396 in wider set of locations is required to test whether this regression is site- and potentially

397 temporally-specific (as plastic use patterns change), and further analysis following the regression
398 analysis would still be needed to identify the types of polymers observed.

399 ***4.2 Comparing microplastic in the Raritan river and estuary to different potential sources***

400 Larger microplastic from potential sources were collected and analyzed to understand if the
401 observed polymer profiles were similar to those observed in the river and bay. The wastewater
402 influent had the highest concentrations of microplastics while also having the greatest range in
403 concentration (333-2250 microplastic/m^3) compared to wastewater effluent, which frequently
404 had a concentration of <1 microplastic/m^3. This suggests that the treatment plants studied here
405 appear to be generally effective at removing microplastics in the morphologies studied (i.e.,
406 fragments, pellets, sheets), which is consistent with a review of the occurrence and fate of
407 microplastic in WWTP that concluded treatment plants were efficient at removing 72-99.4% of
408 microplastics (Gatidou et al., 2019). Including microfibers would increase the concentrations
409 reported here as other have reported this morphology to be prevalent in wastewater effluent.
410 Analyzing microplastic in the potential source water samples in the smaller size class was
411 beyond the scope of this study but is recommended for future work given that the smaller size
412 class was more prevalent in surface waters.

413 The storm water concentrations were between 400 and 600 microplastic/m^3. This is lower than a
414 storm water runoff study by Piñon-Colin that analyzed particles in a larger size range (i.e.,
415 greater than 25 μm) and found a range of 12,000-2,054,000 MP/m^3 in runoff from residential,
416 commercial, and industrial land usage (de Jesus Piñon-Colin et al., 2020). Liu et al. sampled
417 storm water retention ponds for microplastic greater than 10 μm and found concentrations of
418 490-22,894 microplastic/m^3 after looking at residential, industrial, and commercial areas (Liu et

al., 2019a). Piñon-Colin completed visual identification under microscope (de Jesus Piñon-Colin et al., 2020) while this and the Liu study used FTIR analysis (Liu et al., 2019b), therefore the higher greater microplastic concentration may be due to site-to-site differences (i.e., differences in land use and frequency of runoff events) and/or an overestimation due to error in visual identification. The smaller size range of this study (500-2000 μm) could be why it falls on the lower end or well below these ranges.

The polymer concentrations and profiles were compared between the sample types with cluster analysis. Storm water from City B was collected near a parking lot in a residential area and City N adjacent to a highway. These samples contained mainly polyethylene and clustered with 63.4% similarity to one another. Storm water from Field P was collected in between three recreational artificial turf fields clustered at 0% similarity to all other samples and was the only sample from this study (storm water, wastewater, surface water) to contain polystyrene. Other studies have observed higher quantities of polystyrene (Fahrenfeld et al., 2019; de Jesus Piñon-Colin et al., 2020). This unique land use may explain why the results were so different from the other storm samples, although collection of more storm water samples is suggested to fully capture the potential diversity of polymers it contains and potential linkages with land use. Including particle morphology as another dimension could potentially differentiate storm and wastewater, but our literature review did not indicate this was useful for differentiating wastewater influent and effluent (Fahrenfeld et al. 2019).

Storm water from City B and City N had 57.9% polymer similarity with surface water from April 11, 2016 and 26.5% similarity with the rest of the surface water. This indicates that storm water is a potentially significant source of microplastic.

4.3 Implications of results for fate & transport of microplastics

One striking result is the tendency for large microplastics to be present in the freshwater end member of the Raritan River while the smaller size class of microplastics was most prevalent in mid-Raritan Bay. This is most prominent in the data collected on April 11th, 2019. Indeed, both locations in the coastal ocean on this date had higher small microplastics concentrations than those in the Raritan's outflow (Figure 2 and 6). The ratio of large microplastics to small microplastics was significantly lower than predicted by a fragmentation model (Cózar et al., 2014) even if including conservative mixing into ocean waters given the observed salinity values. Thus, this suggests that the source of the smaller microplastics is the Hudson River. This is supported by high concentrations of small microplastics in the two outer most surveys on April 11th, 2019 a region dominated by the much larger Hudson River discharge (Chant et al., 2008a).

The breakup of macroplastics into microplastics occurs due to UV radiation, abrasion by sediments and mechanical stress associated with turbulent shears (Hebner and Maurer-Jones, 2020). We note that the smallest turbulent eddies in the Hudson River scale with the Kolmogorov scale (L_k) (Thorpe, 2007) which decreases with increasing turbulent dissipation rates. Based on observed turbulent kinetic eddy dissipation rates in the Hudson (Peters and Bokhorst, 2000). Kolmogorov scale during peak currents is 0.3 mm and falls in the range of the smaller microplastic class we describe above (particles smaller than 0.25 mm were not analyzed in this study). Microplastics larger than L_k would be sheared apart by these small-scale eddies, while those on that scale or smaller would experience weaker stress. The breakup of marine flocs are also limited to L_k (Akers et al., 1987; Winterwerp, 1998) and we suggest the breakup of microplastics may too be controlled by L_k . Moreover, the Hudson River has a much longer residence time (Bolin, 1973), or equivalently the particle mean transit time, than the Raritan

River, due to the Hudson's larger size to river discharge ratio, and microplastics in Hudson will be subject to many more tidal cycles of intense turbulence that ultimately leads to more breakup and the discharge of smaller microplastics to the coastal ocean. In addition, the ability for microplastics to overcome turbulent mixing decreases with decreasing particle size causing smaller microplastics to be more vertically mixed while larger microplastics remain closer to the surface (Cózar et al., 2014; Cohen et al., 2019). This would, given the surface-intensified seaward flow in estuarine systems (MacCready and Geyer, 2010), flush larger microplastics out of the estuary more rapidly than smaller microplastics. Finally, the size range of microplastics in the open ocean's gyres exhibited low concentrations of microplastics under 1 mm (Cózar et al., 2014) and thus these small microplastics that we observe entering the coastal ocean are unlikely to reach the ocean gyres but rather be lost in the coastal ocean due to biological uptake or deposition.

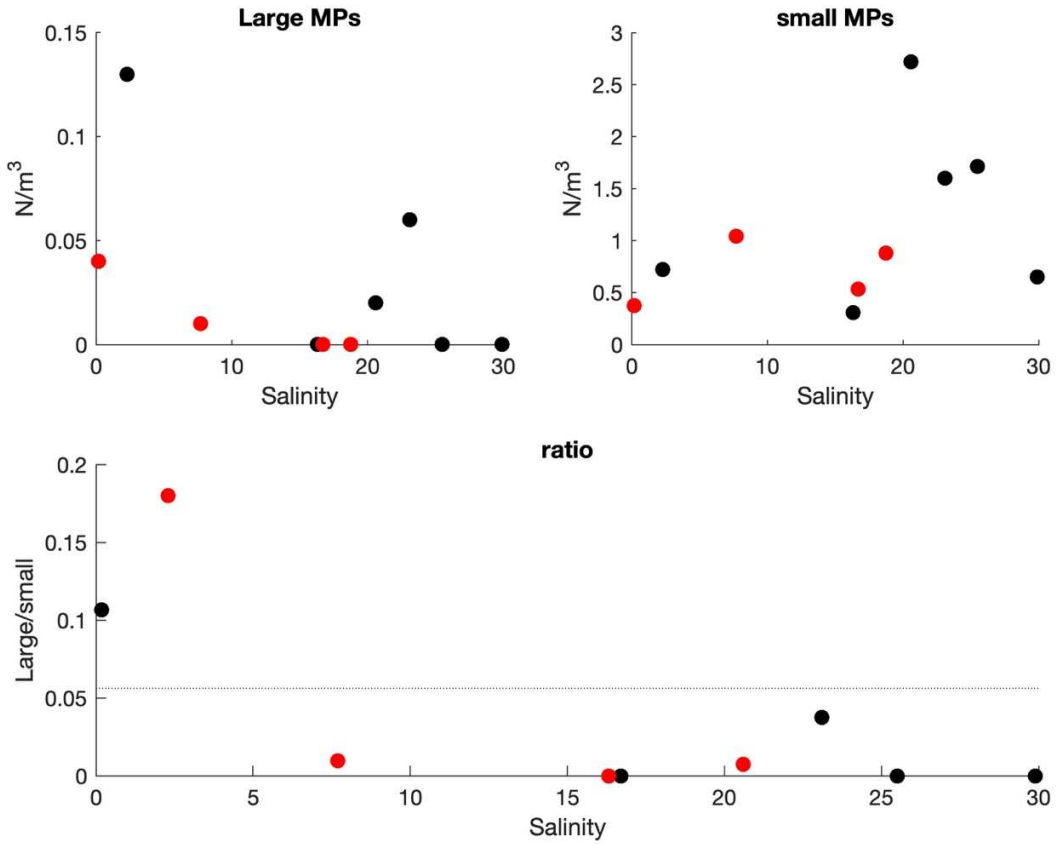

Figure 6 - Large microplastics (MPs) (upper left) and small microplastics (upper right) as function of salinity on April 2019 surveys. Black dots are for 4/11 and red for 4/18. Lower panel shows results of Fragmentation model (Cózar et al., 2014). Dashed horizontal line shows the ratio of large microplastics to small microplastics based on fragmentation.

5. Conclusions

Results provide, to our knowledge, the first characterization of the size distribution of microplastics from a highly urbanized estuarine/coastal system with multiple fresh water inputs, including the Hudson and Raritan Rivers. Relationships were observed between flow conditions and microplastic concentrations with the highest concentrations for 500-2000 μm particles observed during summer low flow conditions at the mouth of the Raritan River. Smaller

489 microplastics (250-500 μm) had higher concentrations in the bay and ocean that likely came
490 from the Hudson River, which has a longer hydraulic residence time. FTIR analyses
491 demonstrated that polyethylene, polypropylene, and rubber were predominant polymer classes
492 observed in the bay. The clustering of storm water polymer results with surface water samples
493 indicated that this understudied pathway of entry is potentially an important source of plastic
494 pollution. A greater number of storm samples with varying land usages would be needed to fully
495 capture the contribution of storm water. Of interest given the analytical burden of identifying
496 microplastics is the observed linear correlation between the total concentration of particles and
497 the microplastic concentration in a sample. Using a regression could reduce analysis time, but a
498 broader set of locations would be needed to further determine this correlation and whether the
499 correlation is site, temporally, or source specific.

500 **Acknowledgements**

501 Funding for this project was provided by the New Jersey Sea Grant (NA18OAR170087).
502 Additional funding was proved by the Rutgers School of Engineering Fellowship to KB and a
503 Hudson River Foundation Tibor T. Polgar Award to KS. Thank you to Dr. Gene Hall for
504 allowing access to his lab's FTIR and to Will Boni, Katie Parrish, and Shreya Patil for lab
505 support. Thanks to Eli Hunter for field support. GAK acknowledges the NJ Higher Education
506 Equipment Leasing Fund (ELF) for FTIR and Raman instrumentation.

507 **6. References**

508

509 Akers, R., Rushton, A., Stenhouse, J., 1987. Floc breakage: the dynamic response of the particle
510 size distribution in a flocculated suspension to a step change in turbulent energy dissipation.
511 Chemical Engineering Science 42, 787-798.

512 Alimi, O.S., Farner Budarz, J., Hernandez, L.M., Tufenkji, N., 2018. Microplastics and
513 nanoplastics in aquatic environments: aggregation, deposition, and enhanced contaminant
514 transport. Environmental Science & Technology 52, 1704-1724.

515 Andrady, A.L., 2011. Microplastics in the marine environment. Marine Pollution Bulletin 62,
516 1596-1605.

517 Atwood, E.C., Falcieri, F.M., Piehl, S., Bochow, M., Matthies, M., Franke, J., Carniel, S.,
518 Sclavo, M., Laforsch, C., Siegert, F., 2019. Coastal accumulation of microplastic particles
519 emitted from the Po River, Northern Italy: Comparing remote sensing and hydrodynamic
520 modelling with in situ sample collections. Marine Pollution Bulletin 138, 561-574.

521 Bolin, B., Rodhe, H. 1973. A note on the concepts of age distribution and transit time in natural
522 reservoirs, Tellus, 25(1), 58-62.

523 Chant, R.J., 2002. Secondary circulation in a region of flow curvature: Relationship with tidal
524 forcing and river discharge. Journal of Geophysical Research: Oceans 107, 14-11-14-11.

525 Chant, R.J., Glenn, S.M., Hunter, E., Kohut, J., Chen, R.F., Houghton, R.W., Bosch, J.,
526 Schofield, O., 2008a. Bulge formation of a buoyant river outflow. Journal of Geophysical
527 Research: Oceans 113.

528 Chant, R.J., Wilkin, J., Zhang, W., Choi, B.-J., Hunter, E., Castelao, R., Glenn, S., Jurisa, J.,
529 Schofield, O., Houghton, R., 2008b. Dispersal of the Hudson River plume in the New York
530 Bight: synthesis of observational and numerical studies during LaTTE. Oceanography 21, 148-
531 161.

532 Cheung, P.K., Cheung, L.T.O., Fok, L., 2016. Seasonal variation in the abundance of marine
533 plastic debris in the estuary of a subtropical macro-scale drainage basin in South China. Science
534 of the Total Environment 562, 658-665.

535 Cheung, P.K., Fok, L., Hung, P.L., Cheung, L.T.O., 2018. Spatio-temporal comparison of
536 neustonic microplastic density in Hong Kong waters under the influence of the Pearl River
537 Estuary. Science of the Total Environment 628-629, 731-739.

538 Choi, B.-J., Wilkin, J.L., 2007. The effect of wind on the dispersal of the Hudson River plume.
539 Journal of Physical Oceanography 37, 1878-1897.

540 Cohen, J.H., Internicola, A.M., Mason, R.A., Kukulka, T., 2019. Observations and Simulations
541 of Microplastic Debris in a Tide, Wind, and Freshwater-Driven Estuarine Environment: the
542 Delaware Bay. Environmental Science & Technology 53, 14204-14211.

543 Convey, P., Barnes, D., Morton, A., 2002. Debris accumulation on oceanic island shores of the
544 Scotia Arc, Antarctica. Polar Biology 25, 612-617.

545 Cózar, A., Echevarría, F., González-Gordillo, J.I., Irigoien, X., Úbeda, B., Hernández-León, S.,
546 Palma, Á.T., Navarro, S., García-de-Lomas, J., Ruiz, A., Fernández-de-Puelles, M.L., Duarte,

C.M., 2014. Plastic debris in the open ocean. Proceedings of the National Academy of Sciences 111, 10239-10244.

de Jesus Piñon-Colin, T., Rodriguez-Jimenez, R., Rogel-Hernandez, E., Alvarez-Andrade, A., Wakida, F.T., 2020. Microplastics in stormwater runoff in a semiarid region, Tijuana, Mexico. Science of the Total Environment 704, 135411.

Desforges, J.-P.W., Galbraith, M., Ross, P.S., 2015. Ingestion of microplastics by zooplankton in the Northeast Pacific Ocean. Archives of Environmental Contamination and Toxicology 69, 320-330.

Estahbanati, S., Fahrenfeld, N.L., 2016. Influence of wastewater treatment plants on microplastics in surface waters. Chemosphere 162, 277-184.

Fahrenfeld, N.L., Arbuckle-Keil, G., Naderi, N., Bartelt-Hunt, S., 2019. Source tracking microplastics in the freshwater environment. TrAC Trends in Analytical Chemistry 112, 248-254.

Franks, P.J., 1992. Sink or swim: Accumulation of biomass at fronts. Marine Ecology Progress Series. Oldendorf 82, 1-12.

Galgani, F., Souplet, A., Cadiou, Y., 1996. Accumulation of debris on the deep sea floor off the French Mediterranean coast. Marine Ecology Progress Series 142, 225-234.

Garvine, R.W., Monk, J.D., 1974. Frontal structure of a river plume. Journal of Geophysical Research 79, 2251-2259.

Gatidou, G., Arvaniti, O.S., Stasinakis, A.S., 2019. Review on the occurrence and fate of microplastics in sewage treatment plants. Journal of Hazardous Materials 367, 504-512.

Hebner, T.S., Maurer-Jones, M.A., 2020. Characterizing microplastic size and morphology of photodegraded polymers placed in simulated moving water conditions. Environmental Science: Processes & Impacts 22, 398-407.

Hitchcock, J.N., Mitrovic, S.M., 2019. Microplastic pollution in estuaries across a gradient of human impact. Environmental Pollution 247, 457-466.

Howell, E.A., Bograd, S.J., Morishige, C., Seki, M.P., Polovina, J.J., 2012. On North Pacific circulation and associated marine debris concentration. Marine Pollution Bulletin 65, 16-22.

Hunter, E.J., Chant, R.J., Wilkin, J.L., Kohut, J., 2010. High-frequency forcing and subtidal response of the Hudson River plume. Journal of Geophysical Research: Oceans 115.

Kapp, K.J., Yeatman, E., 2018. Microplastic hotspots in the Snake and Lower Columbia rivers: A journey from the Greater Yellowstone Ecosystem to the Pacific Ocean. Environmental Pollution 241, 1082-1090.

580 Lam, T.W.L., Fok, L., Lin, L., Xie, Q., Li, H.-X., Xu, X.-R., Yeung, L.C., 2020. Spatial variation
581 of floatable plastic debris and microplastics in the Pearl River Estuary, South China. Marine
582 Pollution Bulletin 158, 111383.

583 Liu, F., Olesen, K.B., Borregaard, A.R., Vollertsen, J., 2019a. Microplastics in urban and
584 highway stormwater retention ponds. Science of the Total Environment 671, 992-1000.

585 Liu, F., Vianello, A., Vollertsen, J., 2019b. Retention of microplastics in sediments of urban and
586 highway stormwater retention ponds. Environmental Pollution 255, 113335.

587 MacCready, P., Geyer, W.R., 2010. Advances in estuarine physics. Annual Review of Marine
588 Science 2, 35-58.

589 Magnusson, K., Eliasson, K., Fråne, A., Haikonen, K., Hultén, J., Olshammar, M., Stadmark, J.,
590 Voisin, A., 2016. Swedish sources and pathways for microplastics to the marine environment.
591 IVL Svenska miljöinstitutet, Stockholm.

592 Mason, S.A., Garneau, D., Sutton, R., Chu, Y., Ehmann, K., Barnes, J., Fink, P., Papazissimos,
593 D., Rogers, D.L., 2016. Microplastic pollution is widely detected in US municipal wastewater
594 treatment plant effluent. Environmental Pollution 218, 1045-1054.

595 Masura, J., Baker, J.E., Foster, G.D., Arthur, C., Herring, C., 2015. Laboratory methods for the
596 analysis of microplastics in the marine environment: recommendations for quantifying synthetic
597 particles in waters and sediments. NOAA Technical Memorandum NOS-OR&R-48.

598 Morritt, D., Stefanoudis, P.V., Pearce, D., Crimmen, O.A., Clark, P.F., 2014. Plastic in the
599 Thames: a river runs through it. Marine Pollution Bulletin 78, 196-200.

600 Nel, H.A., Sambrook Smith, G.H., Harmer, R., Sykes, R., Schneidewind, U., Lynch, I., Krause,
601 S., 2020. Citizen science reveals microplastic hotspots within tidal estuaries and the remote
602 Scilly Islands, United Kingdom. Marine Pollution Bulletin 161, 111776.

603 O'Donnell, J., Marmorino, G.O., Trump, C.L., 1998. Convergence and downwelling at a river
604 plume front. Journal of Physical Oceanography 28, 1481-1495.

605 Peters, H., Bokhorst, 2000. Microstructure observations of turbulent mixing in a partially mixed
606 estuary, I: Dissipation rate. Journal of Physical Oceanography 30, 1232-1244.

607 Pirc, U., Vidmar, M., Mozer, A., Kržan, A., 2016. Emissions of microplastic fibers from
608 microfiber fleece during domestic washing. Environmental Science and Pollution Research 23,
609 22206-22211.

610 Primpke, S., Wirth, M., Lorenz, C., Gerdts, G., 2018. Reference database design for the
611 automated analysis of microplastic samples based on Fourier transform infrared (FTIR)
612 spectroscopy. Analytical and Bioanalytical Chemistry 410, 5131-5141.

613 Rech, S., Macaya-Caquilpán, V., Pantoja, J., Rivadeneira, M., Madariaga, D.J., Thiel, M., 2014.
614 Rivers as a source of marine litter–a study from the SE Pacific. Marine Pollution Bulletin 82, 66-
615 75.

616 Rios, L.M., Jones, P.R., Moore, C., Narayan, U.V., 2010. Quantitation of persistent organic
617 pollutants adsorbed on plastic debris from the Northern Pacific Gyre's "eastern garbage patch".
618 Journal of Environmental Monitoring 12, 2226-2236.

619 Sadri, S.S., Thompson, R.C., 2014. On the quantity and composition of floating plastic debris
620 entering and leaving the Tamar Estuary, Southwest England. Marine Pollution Bulletin 81, 55-
621 60.

622 Scales, K.L., Miller, P.I., Hawkes, L.A., Ingram, S.N., Sims, D.W., Votier, S.C., 2014.
623 REVIEW: On the Front Line: frontal zones as priority at-sea conservation areas for mobile
624 marine vertebrates. Journal of Applied Ecology 51, 1575-1583.

625 Schmidt, N., Thibault, D., Galgani, F., Paluselli, A., Sempéré, R., 2018. Occurrence of
626 microplastics in surface waters of the Gulf of Lion (NW Mediterranean Sea). Progress in
627 Oceanography 163, 214-220.

628 Talvitie, J., Heinonen, M., Pääkkönen, J.-P., Vahtera, E., Mikola, A., Setälä, O., Vahala, R.,
629 2015. Do wastewater treatment plants act as a potential point source of microplastics?
630 Preliminary study in the coastal Gulf of Finland, Baltic Sea. Water Science and Technology 72,
631 1495-1504.

632 Thorpe, S.A., 2007. An introduction to ocean turbulence. Cambridge University Press
633 Cambridge.

634 Wagner, M., Scherer, C., Alvarez-Muñoz, D., Brennholt, N., Bourrain, X., Buchinger, S., Fries,
635 E., Grosbois, C., Klasmeier, J., Marti, T., 2014. Microplastics in freshwater ecosystems: what we
636 know and what we need to know. Environmental Sciences Europe 26, 1.

637 Winterwerp, J.C., 1998. A simple model for turbulence induced flocculation of cohesive
638 sediment. Journal of Hydraulic Research 36, 309-326.

639 Wu, N., Zhang, Y., Zhang, X., Zhao, Z., He, J., Li, W., Ma, Y., Niu, Z., 2019. Occurrence and
640 distribution of microplastics in the surface water and sediment of two typical estuaries in Bohai
641 Bay, China. Environmental Science: Processes & Impacts 21, 1143-1152.

642 Yonkos, L.T., Friedel, E.A., Perez-Reyes, A.C., Ghosal, S., Arthur, C.D., 2014. Microplastics in
643 Four Estuarine Rivers in the Chesapeake Bay, U.S.A. Environmental Science & Technology 48,
644 14195-14202.

645 Zhang, J., Zhang, C., Deng, Y., Wang, R., Ma, E., Wang, J., Bai, J., Wu, J., Zhou, Y., 2019.
646 Microplastics in the surface water of small-scale estuaries in Shanghai. Marine Pollution Bulletin
647 149, 110569.

648